Heliyon 10 (2024) e40976

Contents lists available at ScienceDirect

Heliyon

journal homepage: www.cell.com/heliyon

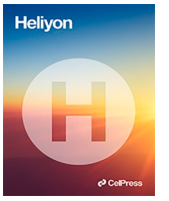

Research article

Extraction of wood vinegar from bagasse and its application as bio-reducer to produce stable silver nanoparticles with enhanced antibacterial activity

M. Ahasanur Rabbi [a,*], Rasheda Akter [a], Most. Halima Khatun [a], Firoz Ahmed [a], Hurey Jahan Kadri [a], Bijoy Maitra [a], M. Zia Uddin Rasel [a], Md. Al-Amin [a], Syed Rashel Kabir [b], M. Rowshanul Habib [b]

[a] *BCSIR Rajshahi Laboratories, Bangladesh Council of Scientific and Industrial Research (BCSIR), Rajshahi, 6206, Bangladesh*
[b] *Department of Biochemistry and Molecular Biology, Rajshahi University, Rajshahi, 6205, Bangladesh*

ARTICLE INFO

Keywords:
Silver nanoparticles
Wood vinegar
Antibacterial activity
Polyphenols
Anticancer activity

ABSTRACT

Global efforts have been made to address environmental and health concerns by promoting and adopting renewable natural resources. This study investigated the role of bagasse-based wood vinegar to synthesize and stabilize silver nanoparticles. We present a simple bottom-up approach to produce silver nanoparticles using the green reducing agent. Wood vinegar has been used to create and stabilize nanoparticles as well as increase the biological activity of silver nanoparticles. In the WV-AgNPs aqueous dispersion's absorption spectra, a wide surface plasmon resonance (SPR) peak with a 395 nm wavelength center was visible. Wood vinegar has been utilized not only to synthesize and stabilize nanoparticles, but it also makes silver nanoparticles biologically more active. Prepared WV-AgNPs showed remarkable antibacterial activity against three pathogenic bacteria and satisfactory antiproliferative activity against human breast (MCF-7) cell line. The stability of the prepared nanoparticles has been confirmed by zeta potential value. The surface morphology and the particle size were investigated by scanning electron microscope and transmission electron microscope. The prepared particles are spherical in shape and particle size ranges from 20 to 40 nm. WV-AgNPs are further characterized by UV–Vis spectroscopy, X-ray diffraction (XRD), Thermogravimetric analysis (TGA), Dynamic Light Scattering (DLS), Energy-dispersive X-ray spectroscopy (EDX) and Fourier transform infrared (FTIR) spectroscopy. Based on the results, it can be concluded that silver nanoparticles mediated by wood vinegar showed promising properties and might find application in the biological domain.

1. Introduction

The development of nanoscience and nanotechnology in almost every field of science has made life easier. The creation of nanomaterials using chemical, physical, and environmentally friendly synthesis techniques is the subject of intense research activities. Recently, there have been significant shifts in researchers' interest in green nanotechnology due to its environmental remediation. Green nanotechnology can improve the environmental remediation process by enhancing existing methods, developing new solutions,

* Corresponding author.
E-mail addresses: rabbi_chem@yahoo.com, ahasanurrabbi@bcsir.gov.bd (M.A. Rabbi).

https://doi.org/10.1016/j.heliyon.2024.e40976
Received 15 July 2024; Received in revised form 27 November 2024; Accepted 4 December 2024
Available online 5 December 2024

reducing costs and risks [1]. Applications of green nanotechnology will result in the creation of clean energy, lighter and more durable materials, affordable clean water production, and will be advantageous for medical applications like smart medications and diagnostics [2]. Green nanotechnology promotes the use of current products in the establishment of innovative nanoproducts that are beneficial to the environment [3]. To reduce environmental and health problems globally, renewable natural resources have been promoted and researchers have begun to search for cheaper and effective biological components or molecules that serve as reducing agents [4]. Biomolecules derived from natural sources can be used to coat silver nanoparticles (AgNPs) to make them biocompatible. Alomar *et al.* synthesized AgNPs using *Neurada procumbens* plant extract that have antimicrobial and anticancer properties [5]. In the field of green nanotechnology, one new breakthrough is the creation of the most dependable and environmentally friendly methods for synthesizing nanoparticles. In order to address these issues in this new nanotechnology era, natural sources that function as capping and reducing agents are good options for producing AgNPs [6,7]. Converting plant biomass through a variety of processes, including carbonization, gasification, and pyrolysis, into gaseous, liquid, and solid fuels is an intriguing way to use renewable natural resources [8,9]. The pyrolysis process generates wood vinegar, a highly oxygenated organic liquid, along with charcoal and smoke. Wood vinegar is mostly composed of acetic acid and water, but it also includes a wide range of organic chemical compounds, including alcohols, hydroxyketones, aldehydes, phenols, ethers, esters, sugars, furans, pyrans, and oxygen compounds [10].

More than 200 water-soluble chemicals are present in wood vinegar, which is a complex combination mostly composed of 80–90 % water [11,12]. The main factor influencing the chemical constituent of wood vinegar is the raw materials utilized [13]. Composition may vary with the temperature and heating rate also [14,15]. Whatever the source and pyrolysis conditions the wood vinegar generally contains high levels of phenolic compounds. 30–60 % of the total organic chemicals in walnut shell wood vinegar are phenolic components [16]. According to previous study wood vinegar from Litchi chinensis contains more than 70 % phenolic compounds [17]. Phenols are mainly produced as the carbonization products of lignin. Breakage of ether linkages among the lignin units and the dehydration reaction of hydroxy groups in propane side chains results in the phenolic compounds [18,19]. Therefore, it can be assumed that biomass with high lignin content will yield wood vinegar with high phenolic compounds.

In agriculture, wood vinegar has been widely utilized, mostly for enhancing soil quality, encouraging the development of plants like fruit trees and vegetables, enhancing the flavor and quality of fruits, and substituting artificial pesticides. Wood vinegar is a novel kind of environmentally friendly natural product that breaks down quickly and has antibacterial and insecticidal properties due to its active phenolic compounds and acids. Wood vinegar is derived from a naturally occurring agricultural product that has no harmful impact on people or animals and does not pollute the environment. As a result, the benefits of wood vinegar have been acknowledged and appreciated over time.

Moreover, a lot of reports were found on the antifungal and antibacterial activities of wood vinegar [20–23]. Considering the abundance of phenolic compounds and their antimicrobial properties, the present work aimed to produce wood vinegar mediated silver nanoparticles (WV-AgNPs). Wood vinegar rich in phenolic compounds can easily reduce metal ions and due to its own antimicrobial activity, metal nanoparticles are likely to exhibit high antimicrobial activity. New biomolecules that can be used to produce nanoparticles will play an important role in green synthesis. Keeping all these points in mind, in this study wood vinegar was produced by pyrolysis from sugarcane bagasse which was subsequently used in the preparation of silver nanoparticles. Wood vinegar mediated silver nanoparticles were further characterized and their antibacterial and anticancer activities were studied.

2. Experimental

2.1. Materials

Sugarcane bagasse was collected form the Harian Sugar mill, Rajshahi, Bangladesh. All compounds used in this research project were of reagent grade purity. We bought sodium hydroxide, silver nitrate from Merck, Germany. Bacterial strains *Escherichia coli,*

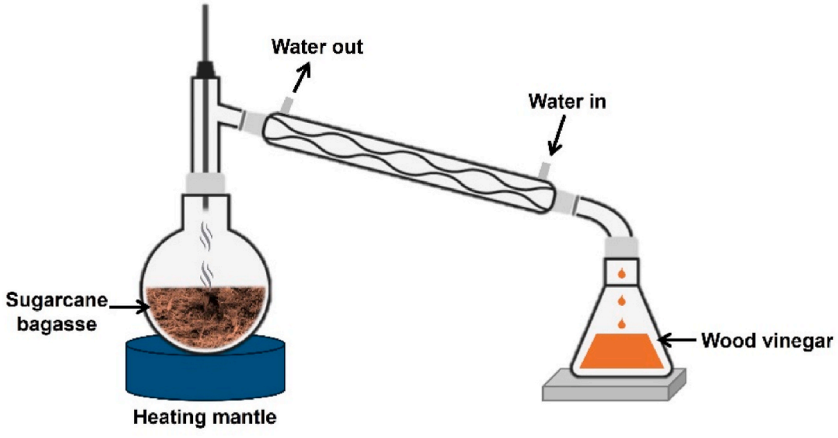

Fig. 1. Production of wood vinegar from sugarcane bagasse.

Shigella boydii, and *Staphylococcus aureus* were collected from Rajshahi University (Department of Biochemistry and Molecular Biology).

2.2. Production of wood vinegar

Preparation, purification, and characterization of sugarcane bagasse-based wood vinegar are described in our previous work [10]. The sugarcane bagasse was cleaned to remove any other fiber or dirt particles. Bagasse was first sun dried and then kept in a heating oven at 80 °C for 24 h. After completely drying, 25 g of bagasse was taken in a single neck round bottom flask. The round bottom flask was heated in a heating mantle and a condenser was connected to the round bottom flask. Sugarcane bagasse was heated at 300–400 °C and the smoke of the burnt bagasse condensed at the condenser. Smoky flavored wood vinegar was collected in a conical flask at the end of the condenser (Fig. 1).

2.3. Purification of wood vinegar

During the pyrolysis process heavy, black, oily portions known as wood tar were also produced along with brown color wood vinegar. The tar decants in the bottom of the container and separates from the WV after a set amount of time, which can range from hours to days to weeks. The crude wood vinegar was filtered after 10 days to remove the insoluble black tar. A clear brown color wood vinegar sample was kept in the refrigerator.

2.4. Synthesis of WV-AgNPs

10 mL of wood vinegar sample was diluted 2 times with distilled water. Then 20 mL of 1M NaOH solution was added to this dilute wood vinegar sample. Now the mixture was stirred well in a magnetic stirrer at room temperature. After 5 min, 100 mL of 0.01M silver nitrate ($AgNO_3$) solution was added slowly to this wood vinegar mixture with continuous stirring. The mixture turns into a deep black color indicating the formation of wood vinegar mediated silver nanoparticles (WV-AgNPs). To purify the particles, WV-AgNPs were centrifuged at 10,000 rpm. The sediment was redispersed in distilled water and centrifuged again. WV-AgNPs were repeatedly washed until the supernatant became clear and the pH of the supernatant became 7.

2.5. Characterization of WV-AgNPs

With a UV–visible spectrophotometer (SP-UV-500DB, Germany), diluted wood vinegar solution and diluted dispersion of WV-AgNPs were examined in spectrum scan mode at wavelengths ranging from 200 to 800 nm. FTIR spectra were recorded in a FTIR spectrophotometer (PerkinElmer, L1600300, UK) including a pyroelectric detector of exceptional sensitivity and linked to PerkinElmer Spectrum IR software version 10.6.2. Samples were placed directly to ATR and spectra recorded between 400 and 4000 cm^{-1} with 16 scans and 4 cm^{-1} resolution and corrected against the background spectrum. JSM-IT800is (JEOL, Japan) was used to take ultra-high resolution SEM pictures. The samples were gold coated using a smart coater (DII-29030-SCTR) before being imaged using a SEM. SEM image of WV-AgNPs were obtained with a working voltage range of 5–25 kV. An EDX spectroscopy adapter that was built-in to the SEM was used to record the EDX spectra. The thermal property of WV-AgNPs sample was investigated by TGA (STA 8000, PerkinElmer, Netherlands). The required amount of WV-AgNPs powder sample heated at a rate of 20 °C min^{-1} in an inert nitrogen environment and the mass loss in percentages was measured. TEM images obtained with the Taalos F 200X TEM from Thermofisher Scientific were utilized to characterize the size and shape of the synthesized WV-AgNPs. Applying a drop of colloidal dispersion to a 300-mesh copper (Cu) grid covered with carbon film and allowing the solvent to evaporate in the air at room temperature was how the TEM measurement was performed. The size distributions and zeta potential of the particles were investigated using a particle size analyzer. The Horiba analyzer (SZ-100) was utilized to investigate the colloidal dispersion of WV-AgNPs. Particle size is analyzed using dynamic light scattering (DLS) at 25 °C and a scattering angle of 90. Utilizing a scanning XRD (Bruker D8 Advance, Germany), the synthesized particles' XRD patterns were captured. The intensity of the measurements was taken at two values of θ, which varied from 10 to 80°. Here, a position-sensitive detector aperture with a scanning rate of 1° min^{-1} at 25 °C was employed. Software for semi-quantitative phase analysis was used to analyze the diffraction spectrum. This helped to smooth the data, minimize noise, and identify the peaks.

2.6. Antibacterial assay

Using the disc diffusion test method, the synthetic WV-AgNPs' antibacterial effectiveness was assessed [24]. Each sterile petri plate was filled with solid nutrition agar medium, and the cultivated pathogens (0.2 mL) were layered on top. The developing test organism was then meticulously coated with filter paper disks at three different locations, and a single Petri dish was used as a positive control with a standard ceftriaxone (40 μg/disc). Next, a dispersion of WV-AgNPs with three distinct concentrations (18, 27, and 45 μg/disc) was gently dropped onto each disc using a micropipette. After a 4-h sample diffusion period at 4 °C in the refrigerator, these antibacterial test plates were incubated for a full 24 h at 37 ± 1 °C to verify bacterial growth. Each experiment was run in triplicate, and measurements were made in terms of zone of inhibition.

2.7. Anticancer activity of WV-AgNPs

The human breast cancer cell line (MCF-7) was cultured in a 25 cm^2 cell culture flask using Dulbecco's Modified Eagle medium (DMEM) and supplemented with 10 % Fetal Bovine Serum (FBS), neomycin, and streptomycin at 37 °C in 5 % CO2. We conducted subcultures at 80–90 % confluence [25,26]. MTS assay was performed to investigate the antiproliferative activity of WV-AgNPs against MCF-7 cell line. The MTS test was performed following manufacturer's instructions (Promega, USA). Using a 96-well culture plate, 1×10^4 MCF-7 cells were seeded in each well with 150 μL of DMEM media for the MTS test. The plate was then incubated for 24 h at 37 °C in a CO_2 incubator. The ultimate concentration of the test sample was 8–256 μg/mL after successively diluted WV-AgNPs in 50 μL of DMEM media were transferred to each well of the growth plate. After that, the plate was incubated for 48 h at 37 °C in a CO_2 incubator. As controls, wells with just MCF-7 cells and no WV-AgNPs were used. Following the removal of the aliquot from each well, 100 μL of DMEM medium was added. Next, each well received 10 μL of MTS containing phenazine ethosulfate, and the mixture was incubated for 2 h. Furthermore, the absorbance was measured using a micro plate reader equipped with a 490 nm filter. For every concentration, three wells were used, and the reduction of cell growth was calculated using the following equation.

$$\text{Proliferation inhibition ratio } (\%) = (A - B) \times 100/A$$

where A and B designates OD_{490} nm of the cellular homogenate (control) without WV-AgNPs and with WV-AgNPs, respectively.

3. Results and discussion

Absorption spectra of wood vinegar and WV-AgNPs were presented in Fig. 2. Dilute wood vinegar solution (WV) and dispersion of WV-AgNPs were examined in spectrum scan mode to investigate the characteristic absorption bands of phenolic compounds and surface plasma resonance (SPR) respectively. The absorption maximum for wood vinegar was found at around 270 nm. Due to the presence of phenolic compounds and organic acids, wood vinegar gives rise to a peak in this region [27]. The absorption coefficient peak value at 270 nm originated from π-π* transition of the wood vinegar forming molecules such as acetic acid, oxalic acid, lactic acid, citric acid, polyphenols etc. Formation of AgNPs is monitored by surface plasma resonance (SPR), which usually appears between 390 and 450 nm. The aggregates were monitored using the absorbance at longer wavelengths (500–700 nm) [28]. Synthesized particles showed maximum surface plasmon resonance (SPR) at 395 nm, which confirms the formation of WV-AgNPs.

The morphology of the synthesized WV-AgNPs was examined using FE-SEM (Fig. 3). The prepared WV-AgNPs were found to be spherical and almost uniform in shape. Most of the particles were individually identified and all particles are in the nanoparticle size range (below 100 nm). Aggregation has been observed in layers which is a common phenomenon of green synthesized AgNPs [29,30].

The synthesis of silver nanoparticles is confirmed by the energy dispersive X-ray (EDX) examination of WV-AgNPs, which displays the peaks in the spectrum of silver caused by its surface plasmon resonance, which is typically at 3 keV (Fig. 4). The WV-AgNPs' EDX profile revealed signals indicating the production of AgNPs in addition to high signals for carbon (C) and oxygen (O), which may have developed as a result of organic capping agents adhering to the AgNPs' surface. On the other hand, AgNPs showed a greater signal, with a silver atom percentage of 89.03. The elemental mapping of synthesized particles also revealed the presence of a higher amount of Ag along with O, and C [31].

It has become achievable to determine the size, shape, and morphology of nanoparticles using transmission electron microscopy (TEM). Fig. 5(a) reveals that the synthesized silver nanoparticles were mostly spherical in shape and uniformly distributed having sizes 20–40 nm. WV-AgNPs were distributed in a very intriguing way since they were linked to one another and arranged in a regular pattern. Fig. 5(b) is the higher magnification of one of the parts of Fig. 5(a), where it was clearly seen that biomolecules i.e. wood vinegar was adhered to particle surfaces and acted as capping agent [32]. The selected area electron diffraction (SAED) pattern (Fig. 5 (c)) suggested that the prepared WV-AgNPs were polycrystalline as the discrete spots line-up and forms rings due to Bragg reflection from individual crystallite [33].

Fig. 6 displays the X-ray diffractogram of WV-AgNPs. The diffractogram shows four intense peaks from the crystallographic plane

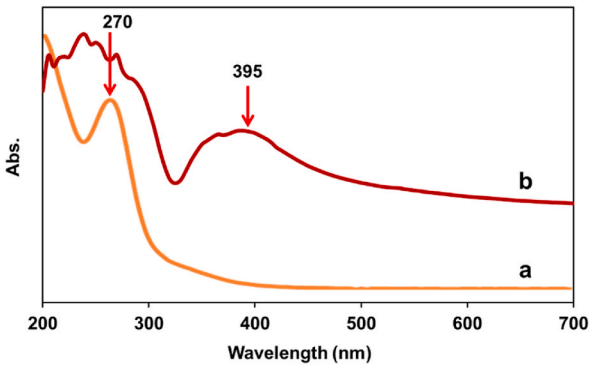

Fig. 2. UV–Vis spectra of (a) wood vinegar and (b) WV-AgNPs.

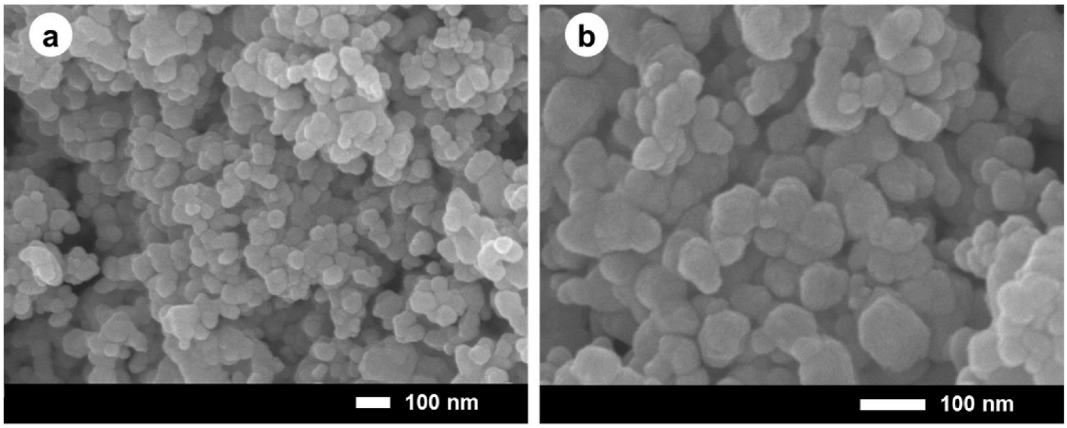

Fig. 3. FE-SEM images of WV-AgNPs at (a) low and (b) high magnification.

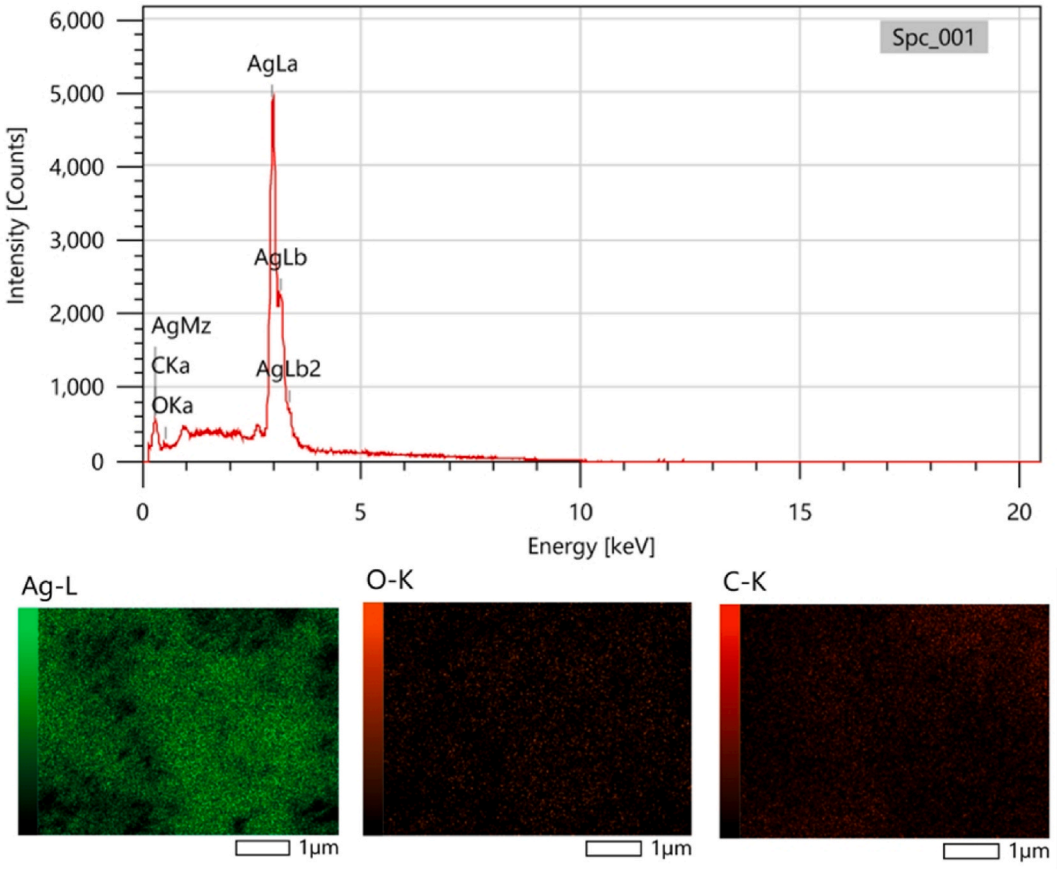

Fig. 4. EDX Spectrum and Elemental mapping of WV-AgNPs.

(111), (200), (220) and (311) at a 2θ value of 38.08°, 44.28°, 64.40° and 77.39° respectively. These peaks are consistent with the face-centered-cubic (FCC) crystal structure of silver nanoparticles (JCPDS No. 89–3722) [34,35]. No extra peak appears in the XRD pattern indicates the formation of pure silver nanoparticle.

FTIR analysis was executed to find out potential functional groups present in the interaction between silver nanoparticles and wood vinegar which was responsible for bio reduction of Ag^{+} and also functioning as capping agent (Fig. 7). The notable broad band peak from FTIR data of WV showed at around 3350 cm^{-1} corresponding to O-H stretching vibration, indicating the presence of phenols [36]. In addition, the peaks approximately at 1638 cm^{-1} for C=O stretching vibration of carbonyl compound, recommending that major constituents in WV were carboxylic acid, aldehyde or ketone due to the pyrolysis of cellulose and hemi-cellulose [37,38], while 1395

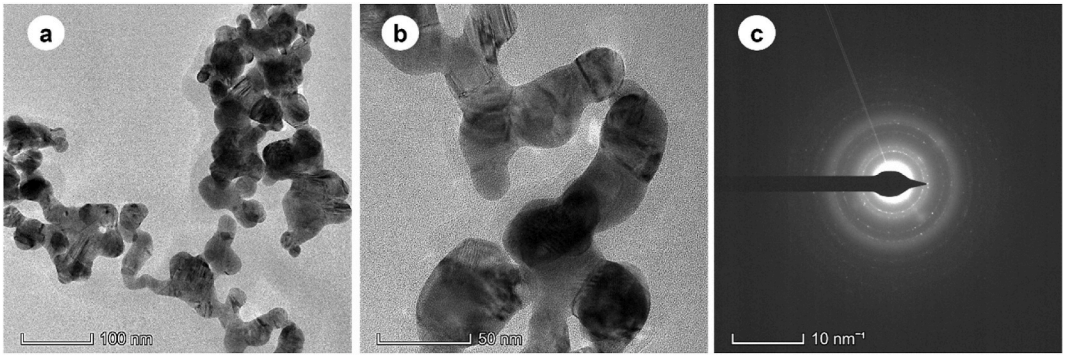

Fig. 5. TEM images of WV-AgNPs at (a) low and (b) high magnifications and (c) SAED pattern.

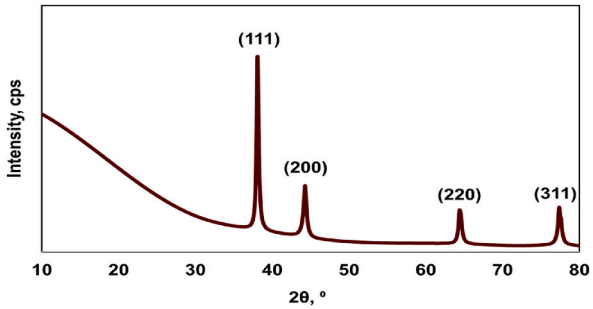

Fig. 6. XRD pattern of WV-AgNPs.

cm^{-1} and 1277 cm^{-1} corresponding to C-O-C and C-O group respectively [39]. The dual character of wood vinegar as reducing and capping agent was confirmed by FTIR spectrum of synthesized silver nanoparticles. The two intense peaks for O-H stretching, C=O stretching vibration were shifted to 3337 cm^{-1} and 1634 cm^{-1}, confirmed the involvement of WV in the synthesis of silver nanoparticles, and some bands were absent, might have been responsible for bio conversion of Ag^{+}. The absence of excess peak in the range of 500–540 cm^{-1}, also supports the free metal ions of silver [40]. Hence, the presence of a highly similar band with small shift, absence of some band in WV-AgNPs compared to the spectrum of wood vinegar (WV), reveals that wood vinegar can act as a reducing agent of Ag^{+} to Ag^{0} and as a stabilizing agent after biosynthesis of AgNPs.

The DLS histogram suggested that the average hydrodynamic diameter of WV-AgNPs was around 94.6 nm (Fig. 8(a)). Normally, DLS is concerned with the diameter of particles suspended in a liquid. DLS does not give the actual size of particles, but rather it provides the size of aggregated particles, which may be different from the actual size of the nanoparticles. This study found that DLS results for biosynthesized WV-AgNPs were larger than SEM and TEM. Because the particle size distribution is not restricted, the

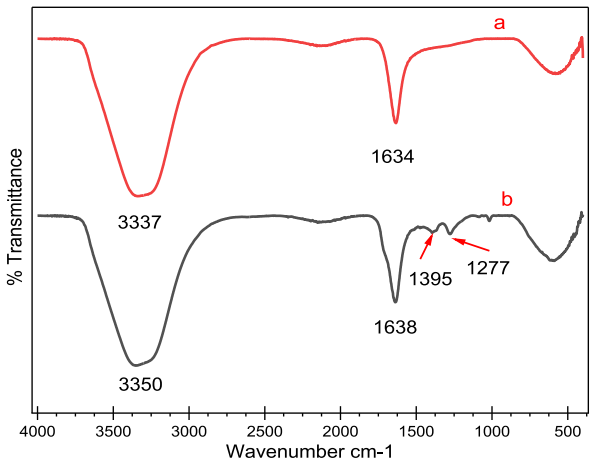

Fig. 7. FTIR Spectra of (a) WV-AgNPs and (b) wood vinegar.

presence of larger particles is likely to result in increased light scattering, causing the observed particle size to shift toward larger values. The polydispersity index (PI) for the colloidal solution of WV-AgNPs is 0.412, which is considered to be of "good" quality, as stated by Liz-Marzán *et al.* [41]. Biosynthesis of AgNPs using wood vinegar as a bio-reducer results in a virtually monodisperse colloidal dispersion of AgNPs. The dispersion was found to be stable, and this finding is in accordance with the stability of colloidal nanoparticles reported in other studies [42]. The surface charge potential, or zeta potential, is a crucial metric to comprehend when analyzing the stability of nanoparticles in aqueous solutions. The physical stability of nano suspensions is enhanced by the electrostatic repulsion of individual particles, which is shown by a large positive or negative value of the nanocrystals' zeta potential. WV-AgNPs' measured zeta potential was −50.2 mV (Fig. 8(b)). Excellent stability behavior of the colloidal solution is indicated by a zeta potential (mV) value greater than ± 60 (mV). Conversely, colloidal solutions with a Zeta potential (mV) value between ± 40 and ±60 (mV) exhibit good stability behavior [43]. We may infer from the findings that biosynthesized colloidal dispersion of WV- AgNPs have good stability.

Thermal stability of WV-AgNPs was investigated using thermogravimetric analysis (TGA). This approach involved gradually raising the temperature to a high of 800 °C from room temperature and measuring the amount of weight lost. The results were displayed on a graph for analysis (Fig. 9). The curve demonstrated an initial mass loss of around 1.0 % at temperatures ranging from roughly 70 °C–200 °C as a result of the sample's water content being removed. Over the temperature range of 300 °C–600 °C, the weight percentage further decreased as the organic components from wood vinegar went away [44]. Up to 800 °C, there was no discernible weight loss over this temperature, and at that point, the residual mass was determined to be 92.3 %. Thus, the high metallic content in WV-AgNPs is responsible for the residual mass (~92.3) of the particles.

The disk diffusion technique was used to assess the antibacterial activity against three types of bacteria. The inhibitory zone diameter was used to represent the results (Fig. 10).

In all bacterial strains, ceftriaxone and WV-AgNPs demonstrated distinct zones of inhibition surrounding the discs. The prepared WV-AgNPs showed potential antibacterial activity against the three bacteria tested, according to the findings of the Agar diffusion experiment. Depending on the WV-AgNP concentration, varying levels of antibacterial activity were observed. There was no discernible change in the activities of WV-AgNPs against gram positive and gram-negative bacteria. Although little higher activities were recorded for gram negative bacteria (*E. coli* and *S. boydii*). Silver nanoparticles' ability to bind to microbe surfaces determines how effective they are [45]. Previous studies have found higher resistance to silver nanoparticles in Gram-positive bacteria than in Gram-negative ones [46,47]. Because of their richer peptidoglycan, the walls of Gram-positive bacteria are more resistant than those of Gram-negative bacteria, which have thin walls with low peptidoglycan content. However, the action of NPs would not be solely dependent on the structure of the bacterial wall [48]. The inhibitory zones for WV-AgNPs range from 8 to 15.5 mm with different particle concentrations. The maximum inhibitory zone (15.5 mm) against *Shigella boydii* is seen at 45 μg/disc WV-AgNPs. Compared to the earlier work [25], WV-AgNPs had relatively excellent antibacterial properties at lower doses. WV-AgNPs were found advantageous over conventional antimicrobial agents as it showed comparable antibacterial activity with ceftriaxone.

The MTS test was used to assess the in vitro cytotoxicity of WV-AgNPs against the MCF-7 cell line. Fig. 11 made it clear that WV-AgNPs might reduce MCF-7 cell viability in a dose-dependent way. After the course of treatment, WV-AgNPs exhibited cytotoxicity to EAC cells at four distinct doses. It turned out that the growth inhibiting impact of WV-AgNPs steadily diminished when concentrations were lowered. At a dose of 256 μg/mL, the highest inhibition (53.67 %) was noted, whereas at a value of 8.0 μg/mL, a minimal inhibition (3.51 %) was recorded. The percentage of inhibition dropped to half of the maximal inhibition when the concentration of WV-AgNPs was 10 times lower than it had been before. Therefore, a significant decrease in growth inhibition caused by a lower dosage of WV-AgNPs was not seen. A prior investigation conducted by Ref. [49] furthermore demonstrated the same kind of outcomes, revealing the cytotoxicity of green-synthesized silver nanoparticles against MCF-7 cells [49]. Additionally, the anticancer efficacy of AgNPs mediated by Potentilla fulgens was evaluated using the MCF-7 cancer cell line [50] wherein MCF-7 was shown to have a 42 % growth inhibition at a dose of 6 μg/mL. AgNPs showed 34.8 % inhibition in this research at a dose of 7.81 μg/mL. AgNPs made from *Bixa orellana* seed extract appeared to be somewhat effective against the MCF-7 cancer cell line when compared to this earlier investigation [25].

4. Conclusion

The current work is among the first to describe the synthesis of silver nanoparticles utilizing wood vinegar derived from sugarcane bagasse. Using a laboratory fixed bed reactor, sugarcane bagasse was pyrolyzed to produce pyrolysis liquid called wood vinegar, which is rich in polyphenols. Using this wood vinegar the green production of AgNPs was effectively completed through wet chemical technique. Ag^{+} was reduced to Ag^{0} by the active phytochemicals in wood vinegar, resulting in a steady dispersion of the silver nanoparticles. Stable monodisperse WV-AgNPs were formed, according to the findings of characterization using UV–visible, XRD, ATR-FTIR, DLS, FE-SEM, EDX, TGA, and TEM methods. WV-AgNPs were discovered to have greater antibacterial activity at comparably lower doses. The smaller size and increased stability of WV-AgNPs may be the cause of better antibacterial activity. Furthermore, wood vinegar's inherent antimicrobial properties may enhance the antibacterial property of WV-AgNPs. Studies on the cytotoxicity of WV-AgNPs against cancer cell lines showed that they were moderately active. In the context discussed above, wood vinegar obtained from biomass has a real potential to be used as bio-reducer to produce stable metal nanoparticles.

CRediT authorship contribution statement

M. Ahasanur Rabbi: Writing – original draft, Methodology, Data curation, Conceptualization. **Rasheda Akter:** Supervision,

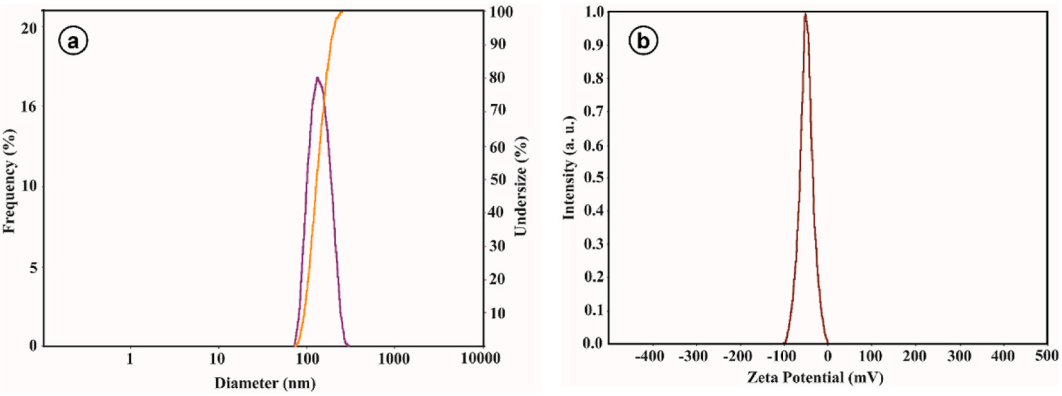

Fig. 8. (a) DLS and (b) Zeta potential distribution histogram of WV-AgNPs.

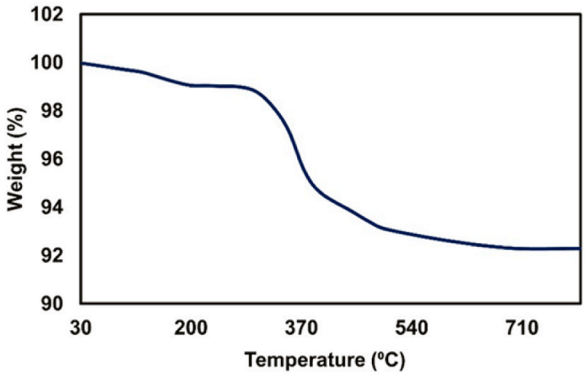

Fig. 9. TGA thermograph of WV-AgNPS.

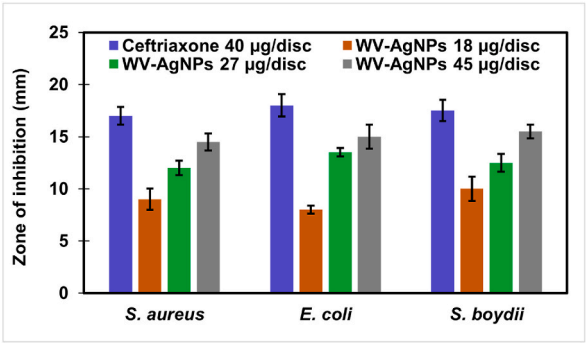

Fig. 10. Antibacterial activities of WV-AgNPs at different concentrations.

Project administration. **Most. Halima Khatun:** Visualization, Validation. **Firoz Ahmed:** Writing – review & editing, Formal analysis, Data curation. **Hurey Jahan Kadri:** Validation. **Bijoy Maitra:** Formal analysis, Data curation. **M. Zia Uddin Rasel:** Visualization, Validation. **Md. Al-Amin:** Formal analysis. **Syed Rashel Kabir:** Investigation. **M. Rowshanul Habib:** Investigation.

Data availability statement

Data will be made available on request; further inquiries may be directed to the corresponding author.

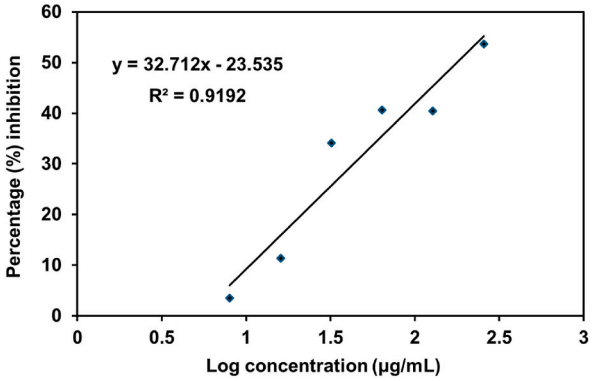

Fig. 11. In vitro growth inhibitory activity of WV-AgNPs against MCF-7 cell line. Each value presented as the mean ± standard deviation from triplicate measurements.

Declaration of competing interest

The authors confirm that they have no conflicts of interest and the data included in this manuscript have not been published previously.

Acknowledgments

This work was supported by Bangladesh Council of Scientific & Industrial Research (BCSIR), Ministry of Science and Technology, People's Republic of Bangladesh.

References

[1] M.L. Del Prado-Audelo, I. García Kerdan, L. Escutia-Guadarrama, J.M. Reyna-González, J.J. Magaña, G. Leyva-Gómez, Nanoremediation: nanomaterials and nanotechnologies for environmental cleanup, Front. Environ. Sci. 9 (2021) 793765, https://doi.org/10.3389/fenvs.2021.793765.
[2] S.S. Salem, A mini review on green nanotechnology and its development in biological effects, Arch. Microbiol. 205 (2023) 128, https://doi.org/10.1007/s00203-023-03467-2.
[3] G.M. Gurtu, M. Sharma, Major applications of green nanotechnology in sustainable development and its impact on global environment: a review, Nat. Volatiles Essent. Oils 8 (4) (2021) 12823–12851.
[4] D. Sharma, S. Kanchi, K. Bisetty, Biogenic synthesis of nanoparticles: a review, Arab. J. Chem. 12 (8) (2019) 3576–3600, https://doi.org/10.1016/j.arabjc.2015.11.002.
[5] T.S. Alomar, N. AlMasoud, M.A. Awad, R.S. AlOmar, N.M. Merghani, M. El-Zaidy, A. Bhattarai, Designing green synthesis-based silver nanoparticles for antimicrobial theranostics and cancer invasion prevention, Int. J. Nanomed. 21 (19) (2024) 4451–4464, https://doi.org/10.2147/IJN.S440847.
[6] A. Chandra, A. Bhattarai, A.K. Yadav, J. Adhikari, M. Singh, B. Giri, Green synthesis of silver nanoparticles using tea leaves from three different elevations, ChemistrySelect 5 (2020) 4239, https://doi.org/10.1002/slct.201904826.
[7] N.K. Sharma, J. Vishwakarma, S. Rai, T.S. Alomar, N. AlMasoud, A. Bhattarai, Green route synthesis and characterization techniques of silver nanoparticles and their biological adeptness, ACS Omega 7 (31) (2022) 27004–27020, https://doi.org/10.1021/acsomega.2c01400.
[8] L.C.D. Medeiros, R.S. Fernandes, C. Sant'Anna, L.H.S. Gasparotto, Dual action of pyroligneous acid in the eco-friendly synthesis of bactericidal silver nanoparticles, Heliyon 8 (11) (2022) e11234, https://doi.org/10.1016/j.heliyon.2022.e11234.
[9] X. Hu, M. Gholizadeh, Biomass pyrolysis: a review of the process development and challenges from initial researches up to the commercialization stage, J. Energy Chem. 39 (2019) 109–143, https://doi.org/10.1016/j.jechem.2019.01.024.
[10] M.A. Rabbi, A. Akhter, M. Khan, H.J. Kadri, B. Maitra, M.H. Khatun, Chemical composition and antifungal activity of sugarcane bagasse and banana stem based wood vinegar, J. Chem. Biol. Phys. Sci. 7 (4) (2017) 898–904, https://doi.org/10.24214/jcbps.D.7.4.89804.
[11] H. Zhou, K. Fu, Y. Shen, R. Li, Y. Su, Y. Deng, Y. Xia, N. Zhang, Physiological and biochemical mechanisms of wood vinegar-induced stress response against tomato Fusarium wilt disease, Plants 13 (2) (2024) 157, https://doi.org/10.3390/plants13020157.
[12] R. Ofoe, L.R. Gunupuru, L. Abbey, Metabolites, elemental profile and chemical activities of *Pinus strobus* high temperature-derived pyroligneous acid, Chem. Biol. Technol. Agric. 9 (2022) 85, https://doi.org/10.1186/s40538-022-00357-5.
[13] R. Xue, E.L. Cui, G.Q. Hu, M.Q. Zhu, The composition, physicochemical properties, antimicrobial and antioxidant activity of wood vinegar prepared by pyrolysis of Eucommia ulmoides Oliver branches under different refining methods and storage conditions, Ind. Crops Prod. 178 (2022) 114586, https://doi.org/10.1016/j.indcrop.2022.114586.
[14] LCD de Medeiros, A.S. Pimenta, R.M. Braga, TK. de A. Carnaval, P.N. Medeiros Neto, DM. de A. Melo, Effect of pyrolysis heating rate on the chemical composition of wood vinegar from Eucalyptus urograndis and Mimosa tenuiflora, Rev. Árvore 43 (4) (2019) e430408, https://doi.org/10.1590/1806-90882019000400008.
[15] A. Grewal, L. Abbey, L.R. Gunupuru, Production, prospects and potential application of pyroligneous acid in agriculture, J. Anal. Appl. Pyrol. 135 (2018) 152–159, https://doi.org/10.1016/j.jaap.2018.09.008.
[16] X. Ma, Q. Wei, S. Zhang, L. Shi, Z. Zhao, Isolation and bioactivities of organic acids and phenols from walnut shell pyroligneous acid, J. Anal. Appl. Pyrol. 91 (2) (2011) 338–343, https://doi.org/10.1016/j.jaap.2011.03.009.
[17] J.F. Yang, C.H. Yang, M.T. Liang, Z.J. Gao, Y.W. Wu, L.Y. Chuang, Chemical composition, antioxidant, and antibacterial activity of wood vinegar from Litchi chinensis, Molecules 21 (2016) 1150, https://doi.org/10.3390/molecules21091150.
[18] Q. Wu, S. Zhang, B. Hou, H. Zheng, W. Deng, D. Liu, W. Tang, Study on the preparation of wood vinegar from biomass residues by carbonization process, Bioresour. Technol. 179 (2015) 98–103, https://doi.org/10.1016/j.biortech.2014.12.026.
[19] C. Amen-Chen, H. Pakdel, C. Roy, Production of monomeric phenols by thermochemical conversion of biomass: a review, Bioresour. Technol. 79 (2001) 277–299, https://doi.org/10.1016/S0960-8524(00)00180-2.

[20] H. Desvita, M. Faisal, Suhendrayatna Mahidin, Antimicrobial potential of wood vinegar from cocoa pod shells (Theobroma cacao L.) against Candida albicans and Aspergillus niger, Mater. Today Proc. 63 (1) (2022) S210–S213, https://doi.org/10.1016/j.matpr.2022.02.410.
[21] F. Misuri, L. Marri, Antibacterial activity of wood distillate from residual virgin chestnut biomass, Eur. J. Wood Prod. 79 (2021) 237–239, https://doi.org/10.1007/s00107-020-01611-z.
[22] X. Hou, L. Qiu, S. Luo, K. Kang, M. Zhu, Y. Yao, Chemical constituents and antimicrobial activity of wood vinegars at different pyrolysis temperature ranges obtained from Eucommia ulmoides Olivers branches, RSC Adv. 8 (2018) 40941, https://doi.org/10.1039/C8RA07491G.
[23] E. de S. Araujo, A.S. Pimenta, F.M.C. Feijó, R.V.O. Castro, M. Fasciotti, T.V.C. Monteiro, K.M.G. de Lima, Antibacterial and antifungal activities of pyroligneous acid from wood of Eucalyptus urograndis and Mimosa tenuiflora, J. Appl. Microbiol. 124 (1) (2018) 85–96, https://doi.org/10.1111/jam.13626.
[24] M.R. Habib, M.R. Karim, Antimicrobial and cytotoxic activity of di-(2-ethylhexyl) phthalate and anhydrosophoradiol-3-acetate isolated from Calotropic gigentia (Linn.) flower, Micobiology 37 (1) (2009) 31–36.
[25] B. Maitra, H. Khatun, F. Ahmed, N. Ahmed, H.J. Kadri, Z.U. Rasel, B.K. Saha, M. Hakim, S.R. Kabir, M.R. Habib, M.A. Rabbi, Biosynthesis of Bixa orellana seed extract mediated silver nanoparticles with moderate antioxidant, antibacterial and antiproliferative activity, Arab. J. Chem. 16 (5) (2023) 104675, https://doi.org/10.1016/j.arabjc.2023.104675.
[26] S.R. Kabir, A.K.M. Asaduzzaman, R. Amin, A.S.M.T. Haque, R. Ghose, M.M. Rahman, J. Islam, M.B. Amin, I.T. Hasan, T. Debnath, B. Chun, X. Zhao, M.K. R. Khan, M.T. Alam, *Zizyphus mauritiana* fruit extract-mediated synthesized silver/silver chloride nanoparticles retain antimicrobial activity and induce apoptosis in MCF-7 Cells through the Fas Pathway, ACS Omega 5 (32) (2020) 20599–20608, https://doi.org/10.1021/acsomega.0c02878.
[27] O. Yalçın, C. Tekgündüz, M. Öztürk, E. Tekgündüz, Investigation of the traditional organic vinegars by UV–VIS spectroscopy and rheology techniques, Spectrochim Acta A Mol Biomol Spectrosc 246 (2021) 118987, https://doi.org/10.1016/j.saa.2020.118987.
[28] F. Dong, E. Valsami-Jones, J.U. Kreft, New, rapid method to measure dissolved silver concentration in silver nanoparticle suspensions by aggregation combined with centrifugation, J. Nanoparticle Res. 18 (2016) 259, https://doi.org/10.1007/s11051-016-3565-0.
[29] M. Ansari, S. Ahmed, A. Abbasi, et al., Plant mediated fabrication of silver nanoparticles, process optimization, and impact on tomato plant, Sci. Rep. 13 (2023) 18048, https://doi.org/10.1038/s41598-023-45038-x.
[30] M. Vanaja, G. Annadurai, *Coleus aromaticus* leaf extract mediated synthesis of silver nanoparticles and its bactericidal activity, Appl. Nanosci. 3 (2013) 217–223, https://doi.org/10.1007/s13204-012-0121-9.
[31] S. Parajuli, P. Nepal, G.P. Awasthi, H.B. Oli, R.L.S. Shrestha, P.L. Homagai, D.P. Bhattarai, Synthesis, characterization and antimicrobial study of silver nanoparticles using methanolic fraction of Artemisia vulgaris leaf, Bibechana 21 (1) (2024) 63–73, https://doi.org/10.3126/bibechana.v21i1.60018.
[32] M. Yilmaz, H. Turkdemir, M.A. Kilic, E. Bayram, A. Cicek, A. Mete, B. Ulug, Biosynthesis of silver nanoparticles using leaves of *Stevia rebaudiana*, Mater. Chem. Phys. 130 (3) (2011) 1195–1202, https://doi.org/10.1016/j.matchemphys.2011.08.068.
[33] S. Li, Y. Shen, A. Xie, X. Yu, L. Qiu, L. Zhang, Q. Zhang, Green synthesis of silver nanoparticles using *Capsicum annuum* L. extract, Green Chem. 9 (8) (2007) 852–858, https://doi.org/10.1039/B615357G, 2007.
[34] S. Sharmin, M.B. Islam, B.K. Saha, F. Ahmed, B. Maitra, M.Z.U. Rasel, N. Quaisaar, M.A. Rabbi, Evaluation of antibacterial activity, in-vitro cytotoxicity and catalytic activity of biologically synthesized silver nanoparticles using leaf extracts of *Leea macrophylla*, Heliyon 9 (2023) e20810, https://doi.org/10.1016/j.heliyon.2023.e20810.
[35] B. Venkatadri, E. Shanparvish, M.R. Rameshkumar, M.V. Arasu, N.A. Al-Dhabi, V.K. Ponnusamy, P. Agastian, Green synthesis of silver nanoparticles using aqueous rhizome extract of Zingiber officinale and Curcuma longa: in-vitro anti-cancer potential on human colon carcinoma HT-29 cells, Saudi J. Biol. Sci. 27 (11) (2020) 2980–2986, https://doi.org/10.1016/j.sjbs.2020.09.021.
[36] L. Liu, X. Guo, S. Wang, L. Li, Y. Zeng, G. Liu, Effects of woodvinegar on properties and mechanism of heavy metal competitive adsorption on secondary fermentation based composts, Ecotoxicol. Environ. Saf. 150 (2018) 270–279, https://doi.org/10.1016/j.ecoenv.2017.12.037.
[37] R. Ríos-Reina, R.M. Callejón, C. Oliver-Pozo, J.M. Amigo, D.L. García-González, ATR-FTIR as a potential tool for controlling high quality vinegar categories, Food Control 78 (2017) 230–237, https://doi.org/10.1016/j.foodcont.2017.02.065.
[38] K.B. Cantrell, P.G. Hunt, M. Uchimiya, J.M. Novak, K.S. Ro, Impact of pyrolysis temperature and manure source on physicochemical characteristics of biochar, Bioresour. Technol. 107 (2012) 419–428, https://doi.org/10.1016/j.biortech.2011.11.084.
[39] A. Mirsoleimani, M. Najafi-Ghiri, H.R. Boostani, et al., Relationships between soil and plant nutrients of citrus rootstocks as influenced by potassium and wood vinegar application, J. Soils Sediments 23 (2023) 1439–1450, https://doi.org/10.1007/s11368-022-03408-4.
[40] K. Ssekatawa, D.K. Byarugaba, C.D. Kato, E.M. Wampande, F. Ejobi, J.L. Nakavuma, M. Maaza, J. Sackey, E. Nxumalo, J.B. Kirabira, Green strategy–based synthesis of silver nanoparticles for antibacterial applications, Front. Nanotechnol. 3 (2021) 697303, https://doi.org/10.3389/fnano.2021.697303.
[41] L.M. Liz-Marzán, M. Giersig, P. Mulvaney, Synthesis of nanosized gold−silica core−shell particles, Langmuir 12 (18) (1996) 4329–4335, https://doi.org/10.1021/la9601871.
[42] K. Kartini, A. Alviani, D. Anjarwati, A.F. Fanany, J. Sukweenadhi, C. Avanti, Process optimization for green synthesis of silver nanoparticles using Indonesian medicinal plant extracts, Processes 8 (2020) 998, https://doi.org/10.3390/pr8080998.
[43] M. Amit, E.V. Ramana, Patents on magnetoelectric multiferroics and their processing by electrophoretic deposition. Recent patents on materials, Science 7 (2) (2014) 109–130, https://doi.org/10.2174/1874464807666140701190424.
[44] A.K. Mittal, J. Bhaumik, S. Kumar, U.C. Banerjee, Biosynthesis of silver nanoparticles: elucidation of prospective mechanism and therapeutic potential, J. Colloid Interface Sci. 415 (2014) 39–47, https://doi.org/10.1016/j.jcis.2013.10.018.
[45] Y.Y. Loo, Y. Rukayadi, M.A.R. Nor-Khaizura, C.H. Kuan, B.W. Chieng, M. Nishibuchi, et al., In Vitro antimicrobial activity of green synthesized silver nanoparticles against selected Gram-negative foodborne pathogens, Front. Microbiol. 9 (2018) 1555.
[46] G. Meroni, J.F. Soares Filipe, P.A. Martino, In vitro antibacterial activity of biological-derived silver nanoparticles: preliminary data, Vet Sci 7 (1) (2020) 12.
[47] M. Torabfam, M. Yuce, Microwave-assisted green synthesis of silver nanoparticles using dried extracts of Chlorella vulgaris and antibacterial activity studies, Green Process. Synth. 9 (1) (2020) 283–293.
[48] M. Mouzaki, I. Maroui, Y. Mir, Z. Lemkhente, H. Attaoui, E.K. Ouardy, R. Lbouhmadi, H. Mouine, Green synthesis of silver nanoparticles and their antibacterial activities, Green Process. Synth. 11 (1) (2022) 1136–1147, https://doi.org/10.1515/gps-2022-0061.
[49] A. Kaler, S. Jain, U.C. Banerjee, Green and rapid synthesis of anticancerous silver nanoparticles by *Saccharomyces boulardii* and insight into mechanism of nanoparticle synthesis, BioMed Res. Int. 2013 (2013) 872940.
[50] A.K. Mittal, D. Tripathy, A. Choudhary, et al., Bio-synthesis of silver nanoparticles using Potentilla fulgens Wall. ex Hook. and its therapeutic evaluation as anticancer and antimicrobial agent, Mater. Sci. Eng. C 53 (2015) 120–127.